

Electron-Phonon Interaction via Electronic and Lattice Wannier Functions: Superconductivity in Boron-Doped Diamond Reexamined

Feliciano Giustino, Jonathan R. Yates, Ivo Souza, Marvin L. Cohen, and Steven G. Louie

*Department of Physics, University of California at Berkeley, Berkeley, California 94720, USA,
and Materials Sciences Division, Lawrence Berkeley National Laboratory, Berkeley, California 94720, USA*

(Received 4 August 2006; published 24 January 2007)

We present a first-principles technique for investigating the electron-phonon interaction with millions of k points in the Brillouin zone, which exploits the spatial localization of electronic and lattice Wannier functions. We demonstrate the effectiveness of our technique by elucidating the phonon mechanism responsible for superconductivity in boron-doped diamond. Our calculated phonon self-energy and Eliashberg spectral function show that superconductivity cannot be explained without taking into account the finite-wave-vector Fourier components of the vibrational modes introduced by boron, as well as the breaking of the diamond crystal periodicity induced by doping.

DOI: [10.1103/PhysRevLett.98.047005](https://doi.org/10.1103/PhysRevLett.98.047005)

PACS numbers: 74.25.Kc, 74.20.-z, 74.25.Jb, 74.62.Dh

The electron-phonon (e -ph) interaction is ubiquitous and plays a central role in a variety of physical phenomena, including finite-temperature electron and spin transport, conventional superconductivity, Peierls instabilities, and polaronic transport in organic materials. Recent advances in synchrotron light sources and electron spectrometers have fostered renewed interest in the e -ph problem. Angle-resolved photoemission spectroscopy [1] nowadays provides information about the momentum and energy dependence of quasiparticle spectra with 2 meV energy resolution and less than 0.01 \AA^{-1} momentum resolution. These recent advances in experimental capabilities define new challenges for theory. However, first-principles calculations of the e -ph coupling are still computationally demanding for simple systems, and far beyond present capabilities for most complex systems [2,3].

The recently discovered superconductivity in boron-doped diamond [4] provides a striking example of a system for which present theoretical methods face severe limitations. Previous investigations on the origin of superconductivity in diamond share the conclusion that pairing is driven by a phonon exchange mechanism [5–9]. However, reported values for the e -ph coupling strength λ show serious inconsistencies, ranging from 0.25 [7] to 0.55 [5], and resulting in transition temperatures spanning 3 orders of magnitude. Most importantly, there remains an unresolved controversy about the very nature of the phonon mechanism involved. One theory argues that the role of the B atoms is to shift the Fermi level in the valence bands of diamond, thereby softening the bulk optical phonons and enabling the e -ph interaction [5–7]. A competing theory supports the notion that the B atoms introduce localized vibrational modes exhibiting anomalously large coupling to electronic states at the Fermi surface [8,9]. Moreover, there exist indications of a possible role of acoustic phonons in the pairing mechanism [9].

In this work, we introduce a first-principles methodology for carrying out robust calculations of the e -ph inter-

action by sampling the Brillouin zone (BZ) with *millions* of k points. This extremely fine sampling, which is necessary in many cases, is achieved by first computing the e -ph vertex in a Wannier representation and then using this result to obtain the matrix elements for arbitrary electron and phonon momenta in the Bloch representation. We demonstrate our technique by investigating the e -ph coupling in superconducting diamond within both a virtual crystal (VC) and a supercell (SC) model with a million points in the BZ. We solve the controversy about the origin of superconductivity by explicitly showing that vibrational modes associated with the B atoms, and particularly the corresponding Fourier components with finite wave vectors, provide an essential contribution to the e -ph coupling strength. On the other hand, the contribution of zone-center phonons is found to be suppressed by the energy conservation selection rule.

The self-energy $\Pi_{\mathbf{q}\nu}(\omega)$ of a phonon with wave vector \mathbf{q} , branch index ν , and frequency $\omega_{\mathbf{q}\nu}$ provides the renormalization and the damping of that phonon due to the interaction with other elementary excitations. Following the Migdal argument, we evaluate the e -ph contribution to the self-energy by replacing the dressed e -ph vertex $\Gamma(1, 2)$ and electron propagator $G(1)$ by their corresponding bare counterparts $g(1, 2)$ and $G_0(1)$, with 1, 2 the quadrimomenta in compressed notation [10]:

$$\Pi(2-1) = -2i \int \frac{d1}{(2\pi)^4} |g(1, 2)|^2 G_0(1)G_0(2). \quad (1)$$

Direct analytical evaluation of Eq. (1) yields [11]

$$\Pi_{\mathbf{q}\nu}(\omega) = 2 \sum_{mn} \int \frac{d\mathbf{k}}{\Omega_{\text{BZ}}} |g_{mn}^\nu(\mathbf{k}, \mathbf{q})|^2 \frac{f_{n\mathbf{k}+\mathbf{q}} - f_{m\mathbf{k}}}{\epsilon_{n\mathbf{k}+\mathbf{q}} - \epsilon_{m\mathbf{k}} - \omega - i\eta}, \quad (2)$$

$\epsilon_{m\mathbf{k}}$ being the energy of an electronic state $|m\mathbf{k}\rangle$ with crystal momentum \mathbf{k} and band index m , $f_{m\mathbf{k}}$ the corresponding Fermi occupation, and η a positive infinitesimal.

The e -ph vertex in Eq. (2) is given by

$$g_{mn,\nu}(\mathbf{k}, \mathbf{q}) = \langle m\mathbf{k} + \mathbf{q} | \Delta V_{\mathbf{q}\nu} | n\mathbf{k} \rangle, \quad (3)$$

where $\Delta V_{\mathbf{q}\nu}$ is the variation of the self-consistent potential induced by a collective ionic displacement corresponding to the vibrational eigenmode $|\mathbf{q}\nu\rangle$. Within the isotropic Eliashberg theory, the spectral function $\alpha^2 F(\omega)$ can be expressed through the imaginary part Π'' of the phonon self-energy in the zero-temperature limit [11,12]:

$$\alpha^2 F(\omega) = -\frac{1}{\pi N_F} \sum_{\nu} \int \frac{d\mathbf{q}}{\Omega_{\text{BZ}}} \frac{\Pi''_{\mathbf{q}\nu}(\omega_{\mathbf{q}\nu})}{\omega_{\mathbf{q}\nu}} \delta(\omega - \omega_{\mathbf{q}\nu}), \quad (4)$$

N_F being the density of states at the Fermi level. Equation (4) establishes the connection between $\Pi_{\mathbf{q}\nu}$ and the e -ph coupling strength $\lambda = 2 \int d\omega \omega^{-1} \alpha^2 F(\omega)$ [11].

At zero temperature, the imaginary part of the phonon self-energy Eq. (2) results in the double delta function $\delta(\epsilon_{n\mathbf{k}}) \delta(\epsilon_{m\mathbf{k}+\mathbf{q}} - \omega)$. While it is customary to neglect the frequency dependence in the second delta function [12], this approximation is not justified in the case of B-doped diamond, as it leads to an artificial divergence of $\Pi_{\mathbf{q}\nu}$ at the zone center [2,3]. In order to incorporate the energy dependence in Eq. (2), η must be chosen smaller than the relevant phonon frequencies, typically $\eta \sim 5$ meV. Correspondingly, the e -ph vertex must be evaluated for millions of inequivalent k points to ensure convergence [3]. While this is beyond existing computational capabilities, such a fine BZ sampling can be achieved by exploiting the localization of electron and phonon Wannier functions.

The maximally localized electronic Wannier functions $|m\mathbf{R}\rangle$ located in the Wigner-Seitz cell \mathbf{R} are obtained from the Bloch eigenstates $|n\mathbf{k}\rangle$ through $|m\mathbf{R}\rangle = \sum_{n\mathbf{k}} e^{-i\mathbf{k}\cdot\mathbf{R}} U_{nm,\mathbf{k}} |n\mathbf{k}\rangle$. The rotation U is found by minimizing the spatial extent of the Wannier states [13]. After evaluating the e -ph vertex $g_{mn,\nu}(\mathbf{k}, \mathbf{q})$ on a coarse BZ grid with Eq. (3), we transform it into the Wannier representation through

$$\langle m\mathbf{0} | \Delta V_{\mathbf{q}\nu} | n\mathbf{R} \rangle = \sum_{\mathbf{k}} e^{-i\mathbf{k}\cdot\mathbf{R}} [U_{\mathbf{k}+\mathbf{q}}^\dagger g_{\nu}(\mathbf{k}, \mathbf{q}) U_{\mathbf{k}}]_{mn}. \quad (5)$$

Since the Wannier functions are strongly localized and the self-consistent potential is local, the quantities $\langle m\mathbf{0} | \Delta V_{\mathbf{q}\nu} | n\mathbf{R} \rangle$ in Eq. (5) decay rapidly with \mathbf{R} . This condition ensures the smoothness of the e -ph vertex in the rotated Bloch basis $U_{\mathbf{k}'} | \mathbf{k}' \rangle$. This allows us to calculate the vertex on a significantly finer mesh of points \mathbf{k}' in the original Bloch space by inverting Eq. (5) [14]. The rotations $U_{\mathbf{k}'}$ needed for the inversion are determined by diagonalizing the Hamiltonian of the system, obtained on the points \mathbf{k}' by similar steps [15].

The procedure here described for the electron momentum \mathbf{k} can be extended with some modifications to the phonon momentum \mathbf{q} . For this purpose we consider the squared e -ph vertex formed by the tensor product of $g_{mn,\nu}(\mathbf{k}, \mathbf{q})$ [Eq. (3)] in the phonon branch index:

$$g_{\mu}^*(\mathbf{k}, \mathbf{q}) g_{\nu}(\mathbf{k}, \mathbf{q}) = \langle \mathbf{q}\mu | \hat{g}_{\mathbf{k}}^2 | \mathbf{q}\nu \rangle. \quad (6)$$

The equality in Eq. (6) is obtained by factoring out the vibrational eigenmodes, while grouping the remainder in the operator $\hat{g}_{\mathbf{k}}^2$. After evaluating the matrix element $\langle \mathbf{q}\mu | \hat{g}_{\mathbf{k}}^2 | \mathbf{q}\nu \rangle$, we transform it in the phonon Wannier representation by using lattice Wannier functions $|\nu\mathbf{R}\rangle$ centered in the Wigner-Seitz cell \mathbf{R} :

$$\langle \mu\mathbf{0} | \hat{g}_{\mathbf{k}}^2 | \nu\mathbf{R} \rangle = \sum_{\mathbf{q}} e^{-i\mathbf{q}\cdot\mathbf{R}} V_{\mathbf{q}}^\dagger g_{\mathbf{k}}^2(\mathbf{q}) V_{\mathbf{q}}. \quad (7)$$

In this case, the rotation $V_{\mathbf{q}}$ is obtained by diagonalizing the dynamical matrix, and the maximally localized lattice Wannier functions simply correspond to the displacement of individual atoms [16]. In most cases, the nonlocality of the operator \hat{g}^2 in real space is short ranged; hence the matrix elements $\langle \mu\mathbf{0} | \hat{g}^2 | \nu\mathbf{R} \rangle$ decay rapidly with \mathbf{R} , and the same procedure adopted for the electronic momentum applies [17]. In some cases, however, such nonlocality may happen to be significant due to the presence of Kohn anomalies, and a denser initial sampling of the vibrational BZ may be required accordingly.

We applied our method to diamond with a boron content of 1.85%, close to the original experimental value [4]. The calculations were performed within the local density approximation to density functional theory [18]. The valence electronic wave functions were expanded in a plane wave basis with a kinetic energy cutoff of 60 Ry, and the core-valence interaction was described by means of norm-conserving pseudopotentials [19,20]. The lattice dynamics was treated within density functional perturbation theory [21], and maximally localized electronic Wannier functions were obtained by minimizing the Berry-phase spatial spread [13,15].

We performed the calculations twice: first for a model VC [6] obtained by generating a $B_x C_{1-x}$ pseudopotential with $x = 1/54 = 0.0185$; second for a $3 \times 3 \times 3$ diamond SC containing 53 C atoms and 1 substitutional B atom [8]. This configuration was chosen since boron-vacancy complexes and boron dimers are either less stable or electrically inactive [22,23]. One possible exception is the 4-boron plus C-vacancy complex which is energetically favored over substitutional boron and acts as a shallow acceptor [22]. This defect, however, has a large activation energy and its study is beyond the scope of this work. The relaxed lattice parameter of the SC model 3.52 Å was employed in all calculations. Electronic and vibrational states were computed by sampling the BZ on $18 \times 18 \times 18$ and $9 \times 9 \times 9$ grids, respectively [24]. These parameters allowed us to reproduce previous results [6,8], thereby validating our setup. By applying our electron and phonon Wannier interpolation, we obtained electronic and vibrational states, as well as e -ph matrix elements, on grids with $100 \times 100 \times 100$ and $30 \times 30 \times 30$ inequivalent electron and phonon crystal momenta, respectively [25]. This sampling ensured the convergence of the phonon self-energy to

within 0.3 meV, with η set to 5 meV and the electronic temperature to 300 K [26].

Figure 1 shows the calculated phonon dispersions corresponding to the VC and to the SC models of B-doped diamond. In the supercell case, we unfolded the small Brillouin zone into its bulk counterpart by projecting the vibrational states on the corresponding bulk eigenmodes with the same wave vector. The VC and the SC phonon dispersions differ most significantly from those of pristine diamond, as well as from each other, for wave vectors smaller than the average Fermi surface diameter $2k_F = 0.93 \text{ \AA}^{-1}$ in the first BZ. The VC model exhibits a smooth softening of the optical branches around the zone center with respect to pristine diamond. The largest softening takes place at the Γ point and amounts to 29 meV (from 165 to 136 meV). Despite the agreement with previous calculations [6,7], these VC values are in sharp contrast with the results of inelastic x-ray scattering on samples with similar doping, reporting a maximum softening of only 7 meV [27]. At variance with the VC model, the SC model shows a milder softening of 14 meV at the zone center (from 165 to 151 meV), in much better agreement with x-ray data, accompanied by the formation of impurity bands at ~ 125 meV (cf. Fig. 1). The flat bands at 151 meV and the impurity bands at 125 meV are in very good agreement with the Raman signals observed in B-doped diamond at 151 and 121 meV, respectively [28].

Figure 2 shows the intensity map of the calculated imaginary part of the phonon self-energy, yielding the phonon full width $\Gamma_{\mathbf{q}\nu} = -2\text{Im}\Pi''_{\mathbf{q}\nu}$. In the VC model, only the vibrational modes with wave vector $q < 2k_F$ exhibit significant linewidths, with values of 13.4 meV close to the zone center. The calculated linewidths of the SC model show smaller values of 9.3 meV around Γ , as well as considerable structure at finite phonon wave vectors, with a maximum of 3.4 meV close to the L point (Fig. 2). Electron-phonon interaction with large momentum transfer

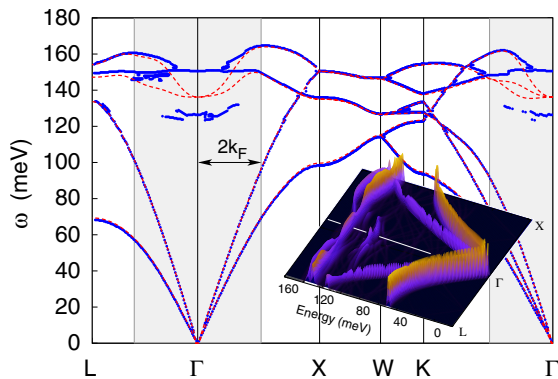


FIG. 1 (color online). Phonon dispersions along the high-symmetry directions of the diamond BZ: VC model (red dashed line) and SC model (blue solid line, from the local maxima of the spectrum in the inset). The modes with $q < 2k_F$ are shaded. Inset: intensity map obtained by unfolding the SC vibrational eigenmodes in the BZ of bulk diamond.

($q > 2k_F$) is actually possible in the SC model. Indeed, the BZ folding reduces the reciprocal space separation between the Fermi surfaces in adjacent zones, thereby allowing umklapp processes. This effect relates to the breaking of the diamond lattice periodicity induced by the doping and is expected to be even more pronounced in a model with a truly random distribution of dopants [29]. Our results are consistent with x-ray data reporting a maximum spectral broadening of 17 meV upon doping [27]. Our calculations also reveal a peculiar suppression of the linewidths and the associated coupling strengths at the zone center: for the optical phonons at Γ we obtained widths of 3.2 and 2.1 meV in the VC and SC models, respectively. The reduced coupling of the electrons to zone-center phonons results from the energy conservation in the scattering process: electronic transitions with no momentum transfer require a minimum energy of ~ 200 meV exceeding the largest phonon frequency of 136 meV. In the present system, this effect is confined within a small BZ spot around the Γ point, which cannot be accessed by x-ray probes. However, a similar mechanism has recently been discussed in relation to the Raman linewidths of MgB_2 [3].

Figure 3 shows the Eliashberg spectral functions calculated from Eq. (4). Both the VC and SC models exhibit peaks in $\alpha^2F(\omega)$ corresponding to van Hove singularities in the optical region of the vibrational spectrum. For the purpose of comparison with previous work [8], we also show in Fig. 3 the Eliashberg function calculated for the supercell model, with the vibrational BZ sampled through the Γ point only (SC_Γ). From the Eliashberg functions we obtained the average e -ph coupling strengths $\lambda_{\text{SC}} = 0.336$, $\lambda_{\text{VC}} = 0.237$, and $\lambda_{\text{SC}_\Gamma} = 0.087$ [30]. The calculated coupling strengths can be used to estimate the superconducting transition temperature through the McMillan equation [11]. In order to make a direct comparison among the

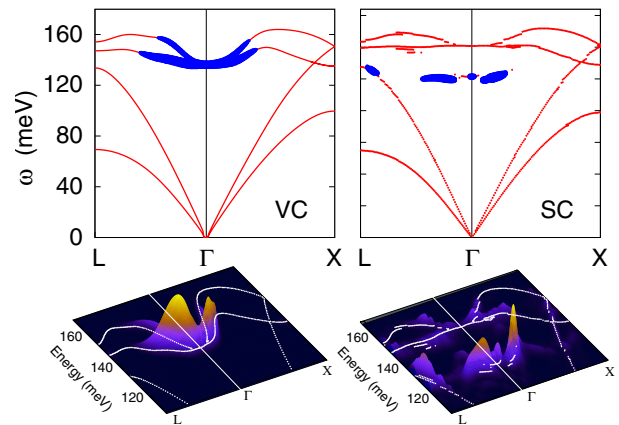


FIG. 2 (color online). Intensity map $\Gamma(\mathbf{q}, \omega)$ of the phonon full widths calculated as $\Gamma(\mathbf{q}, \omega) = \sum_{\nu} \Gamma_{\mathbf{q}\nu} \delta(\omega - \omega_{\mathbf{q}\nu})$. Top: two-dimensional map of the vibrational eigenmodes with full widths > 1 meV (blue disks; the red lines are the phonon dispersions from Fig. 1). Bottom: three-dimensional view of $\Gamma(\mathbf{q}, \omega)$ vs \mathbf{q} and ω (Gaussian broadening of 1 meV). The left (right) panels refer to the VC (SC) model.

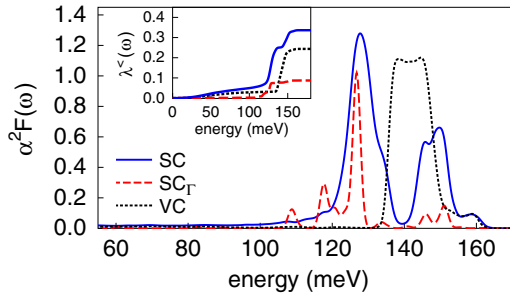


FIG. 3 (color online). Eliashberg function calculated for the SC model (blue solid line), the SC_{Γ} model (red dashed line), and the VC model (black dotted line). Inset: cumulative integral of the Eliashberg function $\lambda^{<}(\omega) \equiv 2 \int_0^{\omega} \alpha^2 F(\omega') / \omega' d\omega'$ showing the contribution of the acoustic modes to λ (about 10% and 20% for the VC and the SC model, respectively).

considered models, we fixed the unknown Coulomb pseudopotential by assigning the experimental transition temperature of 4 K [4] to the SC model. With this choice, we obtained transition temperatures of 0.3 and 0 K for the VC and SC_{Γ} models, respectively. This result clearly indicates that the VC model and the SC_{Γ} model are both *incompatible* with the experimentally observed superconductivity in B-doped diamond. The inadequacy of the VC model [5,6] stems from its inability to account for scattering processes involving large phonon momenta. On the other hand, the SC_{Γ} model [8] misses the dominant contribution to λ arising from the finite-wave-vector Fourier components of the impurity modes.

According to our findings, superconductivity in B-doped diamond cannot be explained without invoking the finite-wave-vector Fourier components of the vibrational modes associated with boron, as well as the breaking of the crystal periodicity induced by doping. More generally, the applications presented here, and especially the large supercell calculation, demonstrate that our new approach to the e -ph interaction is extremely powerful and opens the way to the investigation of many complex problems which are beyond the reach of present computational methods.

This work was supported by the NSF Grant No. DMR04-39768 and by the Director, Office of Science, Office of Basic Energy Sciences, Materials Sciences and Engineering Division, U.S. DOE under Contract No. DE-AC02-05CH11231. Computational resources have been provided by NPACI. Part of the calculations were performed using the QUANTUM-ESPRESSO [31] and WANNIER [32] packages. J. R. Y. and I. S. acknowledge helpful discussions with X. Wang and D. Vanderbilt. F. G. acknowledges helpful discussions with Y.-W. Son and D. Prendergast.

- [1] A. Damascelli, Z. Hussain, and Z.-X. Shen, *Rev. Mod. Phys.* **75**, 473 (2003).
 [2] D. Kasinathan *et al.*, *Phys. Rev. Lett.* **96**, 047004 (2006).
 [3] M. Calandra and F. Mauri, *Phys. Rev. B* **71**, 064501 (2005).

- [4] E. A. Ekimov *et al.*, *Nature (London)* **428**, 542 (2004).
 [5] K. W. Lee and W. E. Pickett, *Phys. Rev. Lett.* **93**, 237003 (2004).
 [6] L. Boeri, J. Kortus, and O. K. Andersen, *Phys. Rev. Lett.* **93**, 237002 (2004).
 [7] Y. Ma *et al.*, *Phys. Rev. B* **72**, 014306 (2005).
 [8] X. Blase, Ch. Adessi, and D. Connétable, *Phys. Rev. Lett.* **93**, 237004 (2004).
 [9] H. J. Xiang *et al.*, *Phys. Rev. B* **70**, 212504 (2004).
 [10] J. R. Schrieffer, *Theory of Superconductivity* (W. A. Benjamin, Inc., New York, 1964).
 [11] G. Grimvall, *The Electron-Phonon Interaction in Metals* (North-Holland, New York, 1981).
 [12] P. B. Allen, *Phys. Rev. B* **6**, 2577 (1972).
 [13] N. Marzari and D. Vanderbilt, *Phys. Rev. B* **56**, 12847 (1997).
 [14] The localization of electronic Wannier functions has recently been exploited to calculate matrix elements of relevance for the anomalous Hall effect: X. Wang *et al.*, *Phys. Rev. B* **74**, 195118 (2006).
 [15] I. Souza, N. Marzari, and D. Vanderbilt, *Phys. Rev. B* **65**, 035109 (2001).
 [16] F. Giustino and A. Pasquarello, *Phys. Rev. Lett.* **96**, 216403 (2006).
 [17] This scheme is closely related to the interpolation of the dynamical matrix via the interatomic force constants: X. Gonze and C. Lee, *Phys. Rev. B* **55**, 10355 (1997).
 [18] D. M. Ceperley and B. J. Alder, *Phys. Rev. Lett.* **45**, 566 (1980); J. P. Perdew and A. Zunger, *Phys. Rev. B* **23**, 5048 (1981).
 [19] N. Troullier and J. L. Martins, *Phys. Rev. B* **43**, 1993 (1991).
 [20] M. Fuchs and M. Scheffler, *Comput. Phys. Commun.* **119**, 67 (1999).
 [21] S. Baroni *et al.*, *Rev. Mod. Phys.* **73**, 515 (2001).
 [22] J. P. Goss and P. R. Briddon, *Phys. Rev. B* **73**, 085204 (2006).
 [23] E. Bourgeois *et al.*, *Phys. Rev. B* **74**, 094509 (2006).
 [24] All quantities referring to the SC model are scaled by $3 \times 3 \times 3$ in order to ensure a size-consistent treatment of the SC and VC models.
 [25] We adopted randomly displaced uniform BZ grids.
 [26] These parameters well describe the zero-temperature limit of $\Pi''_{q\nu}(\omega)$ needed in Eq. (4).
 [27] M. Hoesch *et al.*, *cond-mat/0512424*.
 [28] R. J. Zhang, S. T. Lee, and Y. W. Lam, *Diam. Relat. Mater.* **8**, 1659 (1999).
 [29] The periodic arrangement of dopants in the SC model does not affect our conclusions since the localization length of the impurity modes is shorter than the cell size.
 [30] The value $\lambda = 0.43$ previously obtained for a SC_{Γ} model [8] results from the assumption that the e -ph matrix elements are constant throughout the phonon BZ and equal their corresponding values at Γ , and was evaluated using the double delta-function approximation. On the other hand, our present SC_{Γ} calculation takes the e -ph coupling strengths $\Pi''_{q\nu} / \omega_{q\nu}^2$ constant and equal to their corresponding values at Γ and avoids the double delta-function approximation.
 [31] S. Baroni *et al.*, computer code QUANTUM-ESPRESSO, 2006, <http://www.quantum-espresso.org>.
 [32] A. Mostofi *et al.*, computer code WANNIER, 2006, <http://www.wannier.org/>.